UCRL-JC-130122
PREPRINT

X-ray Spectroscopy from Fusion Plasmas

S. H. Glenzer

This paper was prepared for submittal to the
14th International Conference on Spectral Line Shapes
State College, PA
June 22-26, 1998

August 12, 1998

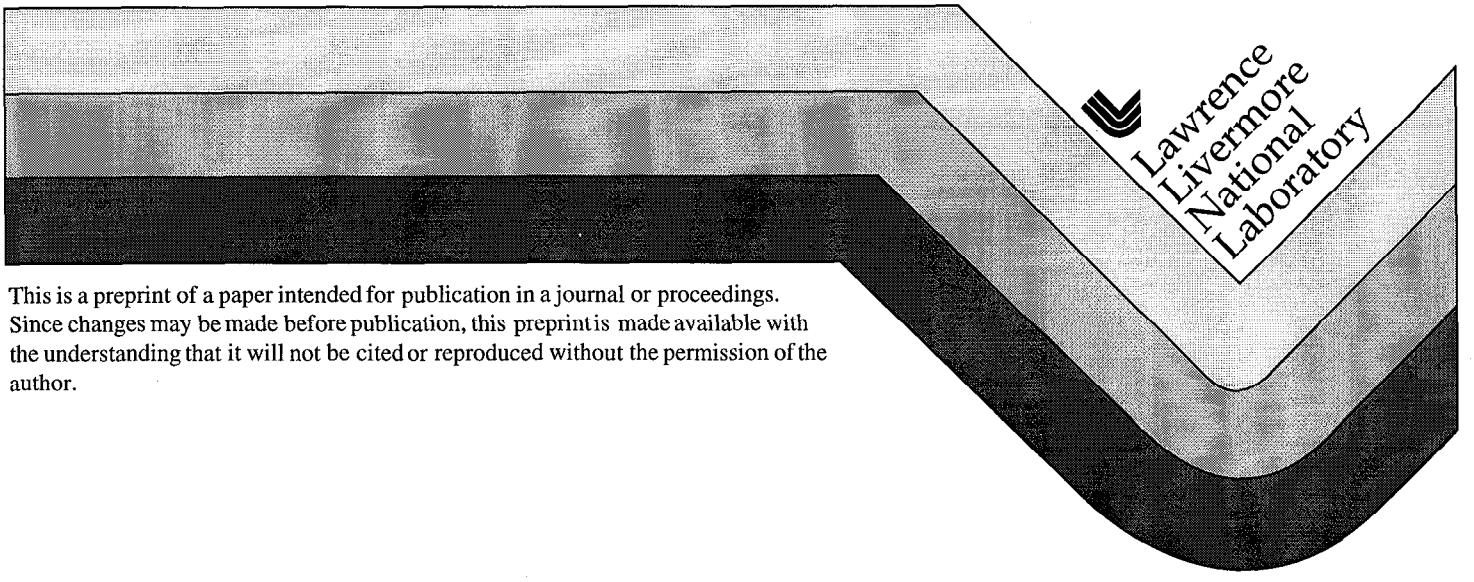

X-ray Spectroscopy from Fusion Plasmas

S. H. Glenzer

Lawrence Livermore National Laboratory, L-399, P.O. Box 808, Livermore, CA 94551

Our understanding of laser energy coupling into laser-driven inertial confinement fusion targets largely depends on our ability to accurately measure and simulate the plasma conditions in the underdense corona and in high density capsule implosions. X-ray spectroscopy is an important technique which has been applied to measure the total absorption of laser energy into the fusion target, the fraction of laser energy absorbed by hot electrons, and the conditions in the fusion capsule in terms of density and temperature. These parameters provide critical benchmarking data for performance studies of the fusion target and for radiation-hydrodynamic and laser-plasma interaction simulations. Using x-ray spectroscopic techniques for these tasks has required its application to non-standard conditions where kinetics models have not been extensively tested. In particular, for the conditions in high density implosions, where electron temperatures achieve 1 - 2 keV and electron densities reach 10^{24} cm^{-3} evolving on time scales of < 1 ns, no independent non-spectroscopic measurements of plasma parameters are available. For these reasons, we have performed experiments in open-geometry gas bag plasmas at densities of 10^{21} cm^{-3} and which are independently diagnosed with Thomson scattering and stimulated Raman scattering. We find that kinetics modeling is in good agreement with measured intensities of the dielectronic satellites of the He-β line (n=1-3) of Ar XVII. Applying these findings to the experimental results of capsule implosions provides additional evidence of temperature gradients at peak compression.

INTRODUCTION

In the indirect drive approach to inertial confinement fusion [1], gas-filled hohlraums are used as radiation enclosures converting high-power laser energy into soft x rays to achieve a symmetric ablation pressure on the fusion capsule and a symmetric high convergence capsule implosion [2]. Present ignition designs for the future National Ignition Facility (NIF) show a significant yield of ~16MJ when absorbing more than 1MJ of laser energy into the hohlraum [2,3]. For this reason, it is crucial to understand backscattering losses by stimulated Brillouin (SBS) and stimulated Raman (SRS) scattering [4,5] since these processes can scatter a significant fraction of the laser energy away from the fusion plasma. Present experiments therefore measure the absolute scattering losses by these processes in addition to the total x-ray production in hohlraums applying various beam smoothing techniques. Smoothing of the laser beams have been shown to reduce

laser scattering losses by suppressing filamentation and hot spots. This result has led to more than 95% absorption of the laser energy in gas-filled hohlraums [6]. Absolute x-ray spectroscopic measurements have shown that 80-90% of the laser light is then converted into x rays which drive the implosion of the fusion capsule.

A small fraction of the laser energy, however, is absorbed into hot electrons [7,8,9]. These electrons have energies in the range of 20 - 40 keV preheating the fusion capsule which in turn results in a reduced capsule compressibility. Calculations show that the time-integrated fraction of hot electrons in an ignition hohlraum must be smaller than 15% (6%) for 20 keV (40 keV) electrons to avoid a reduction of the capsule gain [2]. Applying x-ray spectroscopic measurements of line radiation [10-15] from small tracers have shown that the local hot electron fraction in gas-filled hohlraums is strongly correlated with stimulated Raman scattering [16]. Electron Landau damping of the electron plasma waves which are excited by the stimulated Raman process [17] is the physical mechanism by which these hot electrons have been produced. A peak hot electron fraction of 10% (2% time integrated) has been observed with unsmoothed laser beams indicating the importance to suppress stimulated Raman scattering in fusion targets [16] through the use of beam smoothing techniques as planned on the NIF.

Capsule implosions driven by x rays from high-Z hohlraums converge to a final radius ~10 smaller than the original radius of about 275 μm in present indirect drive experiments. Consequently plasma conditions similar to those of stars of extremely high densities 10^{24} cm^{-3} and temperatures 1 - 2 keV have been produced [18]. The characterization of these dense plasmas requires x-ray or neutron diagnostics. In particular, the spectrum of the He-β line (n=1-3) of Ar XVII with its dielectronic satellites has been found to be a valuable diagnostic of electron densities and temperatures. This line is Stark broadened so that densities can be inferred from the width of the spectral line, and the upper levels of the dielectronic satellites on the red wing of the He-β line are populated by dielectronic recombination so that their relative intensity is sensitive to the electron temperature. The contribution of the satellites is especially important at earlier times in the implosion where temperatures are below 1 keV so that the satellites need to be self-consistently included in the fit of the whole line shape with a Stark-broadening code coupled to a kinetics model. Recent temporally resolved measurements [19] of the spectrum of the He-β line plus satellites have resulted in a density of 10^{24} cm^{-3} and peak temperatures of ~1 keV which are somewhat lower than calculated with two-dimensional hydrodynamic modeling using the code LASNEX. For this reason we have performed new experiments in open-geometry gas bag plasmas [20-22] at densities of 7×10^{20} cm^{-3} and 10^{21} cm^{-3}. These gas bag plasmas are independently diagnosed with spectroscopy [22], Thomson scattering [23], and stimulated Raman scattering [20,24]. In particular, the Thomson scattering diagnostics has been developed to a high degree of accuracy in these fusion plasmas. It is now possible to measure electron temperatures T_e and densities n_e, ion temperatures T_i, macroscopic flow velocities $\mathbf{v}$, and the averaged ionization stage Z. Possible effects due to turbulence as suggested in Ref. [25] can be clearly ruled out from the experimental Thomson scattering spectra [26]. We find that the kinetics modeling is in good agreement with the measured intensities of the dielectronic satellites of the He-β line (n=1-3) of Ar XVII for the two different electron densities. This result verifies the kinetics modeling used for the interpretation of implosion spectra. It

further indicates that the somewhat lower temperature from the satellites might be a combined effect of spatial gradients in the fusion capsule and of the weak intensity of the satellites at peak temperature where Stark broadening introduces great difficulties in determining their intensity.

HOHLRAUM COUPLING EXPERIMENTS

Cylindrical gold hohlraums of 2,750 μm length and 800 μm radius were heated in experiments at the Nova Laser Facility at the Lawrence Livermore National Laboratory [27] applying various beam smoothing techniques. These hohlraums are of the standard size for capsule implosions [18,28] and present benchmarking experiments [29-31] at Nova. On each side five laser beams enter the hohlraum through laser entrance holes (LEH). Besides regular empty hohlraums we shot hohlraums filled with 1 atm of methane (CH_4) and used 0.35 μm thick polyimide to cover holes. A total of ten shaped laser beams were applied with a duration of 2.4 ns rising from a 7 TW foot to 17 TW peak power (pulse shape no. 22: PS22). The total energy supplied to the target was 29 kJ. Experiments were performed with standard unsmoothed Nova beams and with two types of beam smoothing conditions. The beams were smoothed by using Kinoform Phase Plates (KPP) [32-34] which break each beam into many several-mm-scale beamlets whose diffraction limited focal spots are then superposed in the target plane producing an intensity envelope without large scale-length inhomogeneities but consisting of fine scale hot spots (speckles).

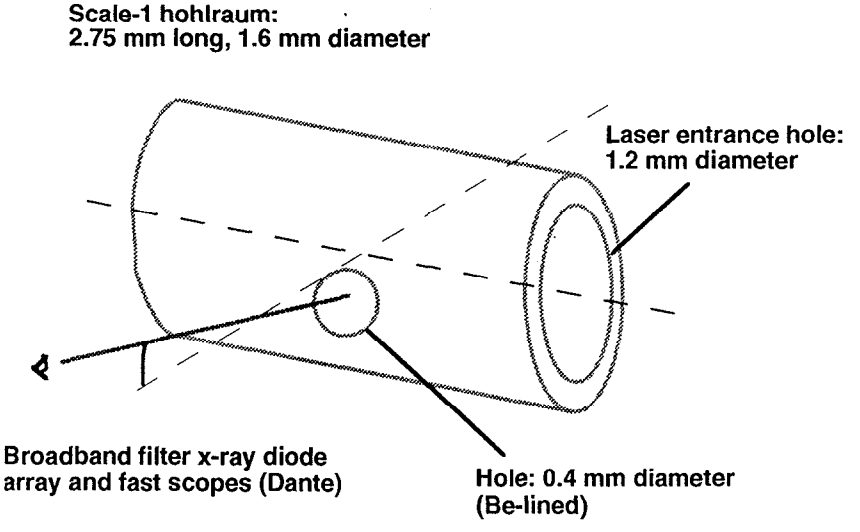

Figure 1. Schematic of a scale-1 Nova hohlraum. The holes are covered with polyimide to contain the gas. The hohlraum temperature is measured through the holes.

The focal spot is further smoothed through use of Smoothing by Spectral Dispersion (SSD) [35,36], where the combination of bandwidth of 0.22 nm at

1ω together with a dispersive grating in the beam line serves to move the speckles in the focal plane on time scales ~5 ps short compared with that required for hot spots to form a filament in the plasma (~10 ps - 20 ps). The present configuration results in peak laser intensities of 2 x 10^{15} W cm^{-2} at the LEH which are comparable to those anticipated in NIF hohlraums.

We measure the x ray production in the hohlraums with a broadband filter x-ray diode array and fast scopes [37]. This instrument detects the radiation flux per steradian temporally and spectrally resolved $\phi(t,\nu)$ emitted along the collimated line of sight from the indirectly heated wall opposite a diagnostic hole (450 μm diameter) in the side of the hohlraum (Fig. 1). The hohlraum wall temperature is then obtained by $\Phi(t) = \sigma T_{wall}^4(t) A_d$, where $\Phi(t)$ is the frequency-integrated radiation flux (0-2 keV) emitted from the wall through a diagnostic hole (area A_d) and σ is the Stefan-Boltzmann constant. Figure 2(a) shows examples of temporally resolved emission spectra of the gold hohlraum wall in the energy range 1 keV - 2 keV. The spectra are integrated over 100 ps. From the absolute power we deduce the hohlraum wall temperature as function of time as plotted in Fig. 2(b). The temperature measurements compare well to the detailed radiation hydrodynamic modeling [6,38-40]. In particular, at the peak of the x-ray drive at $t = t_0 + 1.8$ ns measured and calculated temperatures match well. The calculations use corrected pulse shapes with SBS and SRS losses subtracted. From these wall temperature data it is possible to arrive at an estimate of the hohlraum radiation temperature T_{RAD} [41-44] which is a measure of the total x-ray production in hohlraums and is important for the purpose of simulating capsule implosion dynamics because the capsule is irradiated by x rays from both, the indirectly and directly heated hohlraum wall. This correction, called albedo correction, is performed on calculational basis [40] and corroborated by witness plate measurements [44] and x-ray emission measurements through the laser entrance hole [6,45,46].

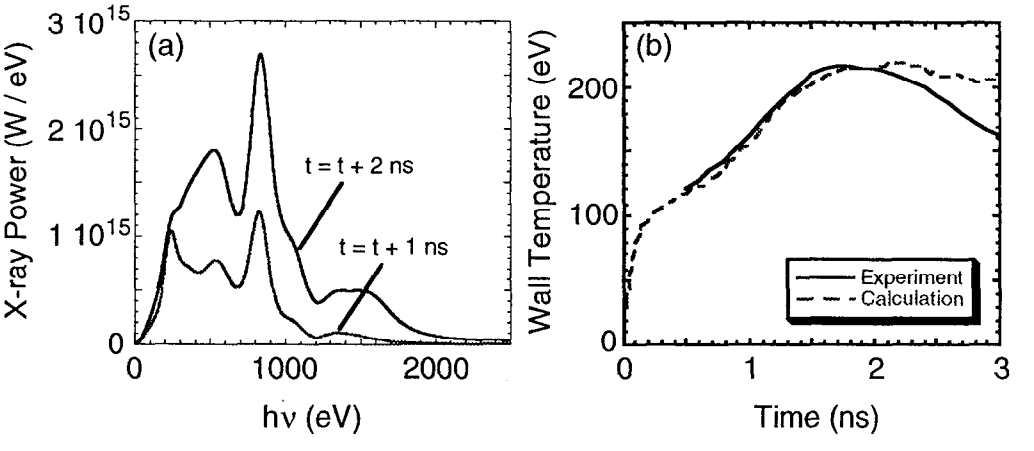

Figure 2. Temporal resolved absolute broadband spectra from the hohlraum gold wall (a) and hohlraum wall temperature as function of time together with LASNEX simulations (b).

Simultaneously, three independent detection systems have been applied for a complete measurement of the scattering losses. Backscattering into the lens of one

of the Nova laser beams has been detected with a full aperture backscattering diagnostic [20]. The light was imaged onto a frosted silica plate and detected temporally and spectrally resolved with filtered diodes, spectrometers, and optical streak cameras. The whole detection system was absolutely calibrated *in situ* by retro-reflecting 8% of a full-power laser shot into the detector. Light scattered at larger angles up to 22° was measured with a near backscattering imager [47] consisting of a calibrated aluminum scatter plate mounted around the lens and two-dimensional imaging detectors for SBS and SRS. Light scattered at larger angles was collected with calibrated diodes.

Figure 3 shows the time-integrated SBS and SRS losses and the experimental wall temperatures of methane-filled and empty hohlraums for various beam smoothing conditions. For gas-filled hohlraums we find that the total scattering losses are reduced from (18 ± 3)% for unsmoothed laser beams to (3 ± 1)% when applying KPPs plus 0.22 nm SSD. Simultaneously, we observe that the temperatures increase by 15 eV. This increase of the hohlraum temperatures for smoothed laser beams is consistent with the reduction of backscatter losses and is clear evidence of improved energy coupling into the hohlraum

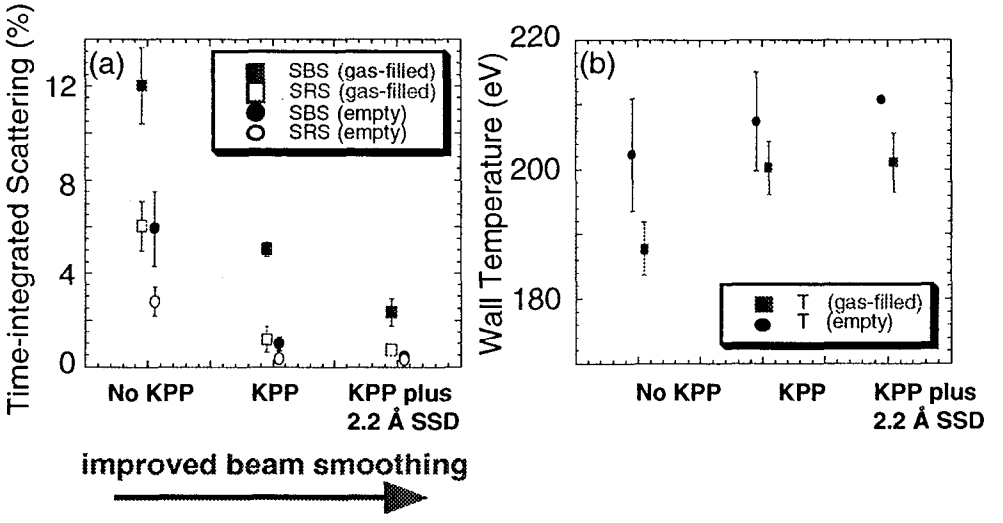

Figure 3. Stimulated scattering losses by SRS and SBS (a) and peak wall temperatures (b) for gas-filled and empty hohlraums.

These experimental observations are consistent with calculations of the filamentation threshold [48,49] and with measured Raman spectra. We observe that short wavelength Raman scattering is gradually suppressed with improved beam smoothing consistent with a reduction of energy in hot spots which produce filamentation (KPP only) and the reduction of the filamentation rate of hot spots (with additional SSD). For our plasma conditions [31], calculations show that the laser beams filament for intensities of $I > 5 - 8 \times 10^{15}$ W cm^{-2}. For unsmoothed laser beams more than 30% of the laser beam exceeds this threshold in the LEH region where Raman scattering occurs. On the other hand, a smoothed laser beam shows a significantly smaller fraction of high intensity spots. Typically less than

5% of a Nova beam smoothed with a KPP is above the filamentation threshold and therefore such beams are more stable against filamentation.

The comparison of the experimental wall temperatures with simulations [6,40] and scalings [2,50] indicate a laser conversion efficiency into x rays of 80% - 90%. This estimate is based on the measured absorbed energy into the hohlraum where SBS and SRS losses are already subtracted. The suppression of these parametric scattering processes is therefore important for the energetics of hohlraums avoiding laser energy losses and consequently maximizing the x-ray production. In addition, it is particularly critical to suppress stimulated Raman scattering because of the production of hot electrons. Stimulated Raman scattering is a three wave process where an incident light wave decays into a scattered light wave of smaller energy and an electron plasma (Langmuir) wave. The electron plasma wave is damped by electron Landau damping where electrons can gain significant energy from the wave turning into so-called hot electrons. The process obeys the Manley-Rowe relations (energy and momentum conservation) from which we can calculate energies of 20-40 keV of the hot electrons for typical parameters of inertial confinement fusion plasmas. These electrons can preheat the fusion capsule reducing its compressibility. Calculations show that for future ignition experiments, e.g., at the National Ignition Facility (NIF), the time-integrated hot electron fraction must be smaller than 15% (6%) for 20 keV (40 keV) electrons to avoid a reduction of the capsule gain.

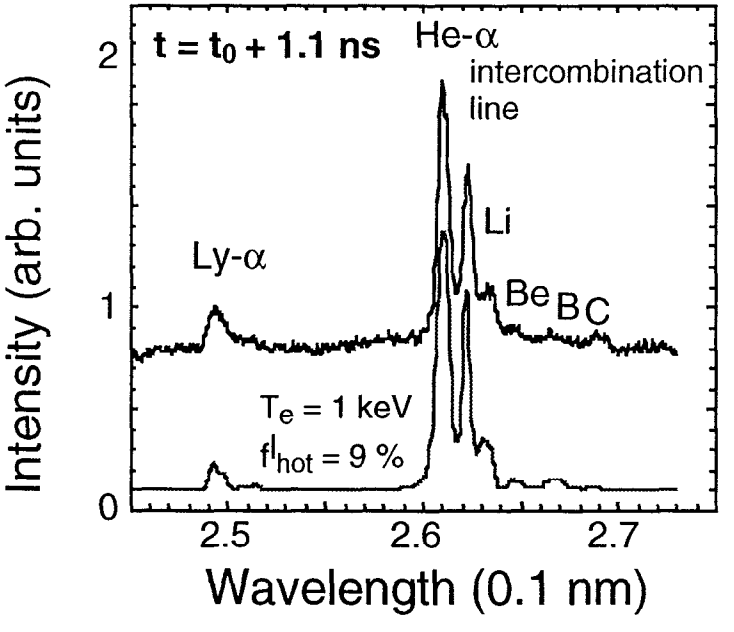

Figure 4. Example of a temporally resolved titanium emission spectrum coated on a tracer foil in a gas-filled Nova hohlraum. A peak hot electron fraction of 9 % is inferred.

We have measured the *local* hot electron fraction in gas-filled hohlraums by x-ray emission spectroscopy using titanium-chromium tracers mounted at various

locations in a gas-filled hohlraum. These hohlraums were heated with unsmoothed Nova beams showing a significant fraction of the total laser energy (E_{tot} = 27 kJ) scattered by stimulated Raman scattering ($E_{SRS} \cong 1$ kJ). These experiments show a clear correlation between the time histories of stimulated Raman scattered light and of the hot electron fraction measured with x-ray spectroscopy. The presence of highly energetic electrons in these plasmas gives rise to characteristic x-ray emission features showing hydrogen-like resonance emission simultaneously with the emission of Li-, Be-, B-, and C-like satellite lines on temporally resolved spectra. An example of a spectrum measured 1.1 ns after the beginning of the 2.4 ns long laser pulse is shown in Figure 4. The intensity of the hydrogen-like resonance transition in Ti (1s ^{2}S - 2p ^{2}P^o or Ly-α) is found to be more than one order of magnitude larger than calculated for a Maxwellian electron velocity distribution function with a temperature obtained from independent measurements. This spectral line together with the emission from lower ionized charged stages can be used to quantify the hot electron fraction.

For our conditions, we can approximate the electron velocity distribution function by a cold thermal Maxwellian distribution (T_e) plus a Maxwellian tail of hot electrons (T_{hot}) produced by SRS [8,9]. A standard spectroscopic tool to infer T_e is the line intensity ratio of the He-α line to the lithium-like dielectronic satellites which are dominated by the jk l dielectronic satellites [51]. Extending the analysis of Ref. [15] to the temperature and density regime encountered in this experiment shows that T_e is high enough so that this method is not sensitive to the presence of hot electrons in the plasma. For example, at $t = t_0 + 1.1$ ns this ratio gives $T_e \cong 1$ keV for the titanium-chromium foil plasma. Complete spectra simulations as shown in Figure 4 and additional measurements of the intensity ratio of the He-β lines from titanium and chromium [52] verify this result. This value is slightly smaller than 1.5 keV of the surrounding CH-plasma as measured with Thomson scattering [31], because the heating of the foil lags behind that of the gas.

The comparison of the experimental spectra with synthetic spectra applying collisional-radiative model calculations shows that the experimental spectra are influenced by hot electron excitation. Including a non-Maxwellian electron velocity distribution function into the modeling gives a quantitative estimate of the plasma conditions. On the other hand, assuming a Maxwellian velocity distribution with temperatures of 1 - 1.5 keV results in a calculated relative intensity of the Ly - α transition which is at least one order of magnitude smaller than experimentally observed (Fig. 4). Using time-dependent non-Maxwellian calculations which include hot electrons with an energy of 20 keV (based on x-ray continuum measurements [10] results in a wider range of ionization stages showing the Ly - α lines, the He - α line, intercombination line, and the Li-, Be-, B-, and C-like n = 2 satellites as observed in the experiments. The calculated spectrum shown in Fig. 4 matches the observed intensities rather well and has been calculated for a hot electron fraction of 9%. This result is valid for unsmoothed Nova beams and is significantly larger than the experimental values obtained for smoothed laser beams. X-ray continuum measurements from gas-filled hohlraums which have been heated with beams smoothed by KPPs plus SSD show that the (time-integrated) hot electron fraction is reduced by a factor of about 10. This finding is consistent with the factor of 6 drop of SRS losses seen in Fig. 3(a) for gas-filled hohlraums.

Figure 5 shows the temporal evolution of the hot electron fraction inferred from the spectra synthesis for spectra measured at various times during the hohlraum heating. The independently measured SRS losses are shown for comparison. A correlation between the hot electron fraction and the SRS signal is apparent. The error bar for the hot electron fraction is in the range of 25% - 50%. Other parameters such as the electron density and opacity are obtained self consistently from the spectra. They compare well with the results of the hydrodynamic modeling and with calculations based on the initial conditions of the experiments. From the temporally integrated spectroscopic hot electron fraction

$$1/T \int_0^{2.4} f_{hot}(t)\, dt \cong 0.2$$

we find an averaged hot electron energy of E_{hot} = 500 J with E_{hot} / E = 0.019 (E = 27 kJ the total laser energy delivered to the hohlraum) assuming that the local value of the hot electron fraction is valid for a large part of the hohlraum plasma and further using an averaged electron density of 10^{21} cm^{-3} from hydrodynamic calculations.

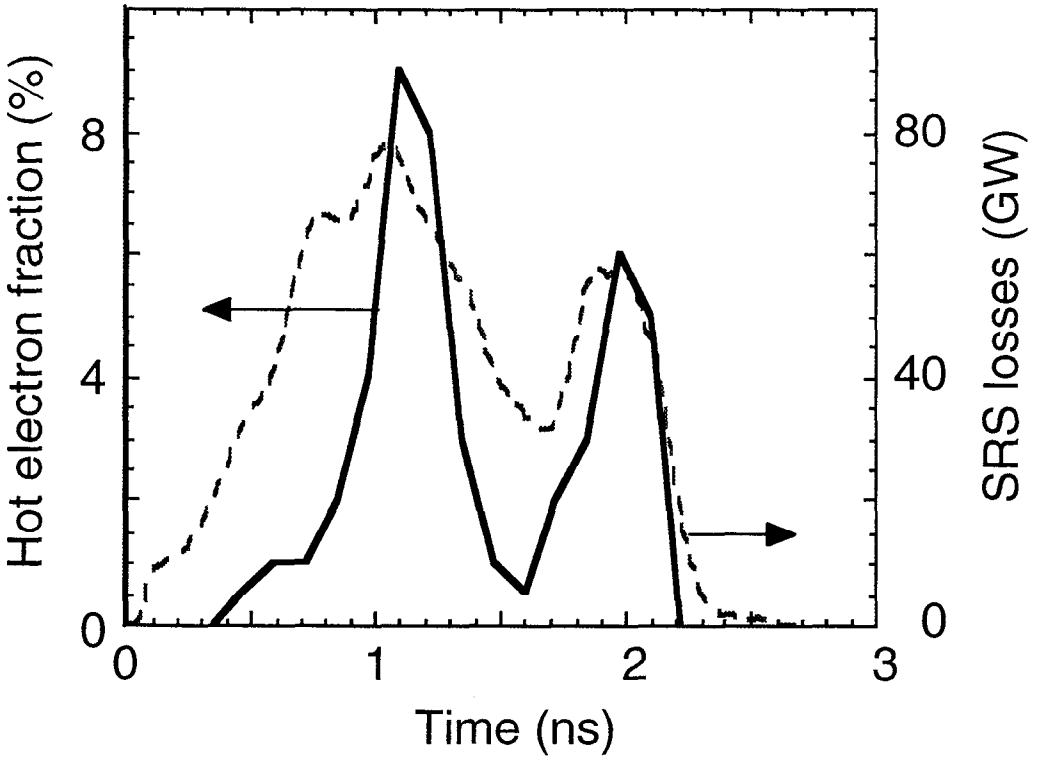

Figure 5. Hot electron fraction from x-ray emission spectroscopy and stimulated Raman scattering losses as function of time. A clear correlation can be observed.

This value for the time-integrated hot electron fraction is in close agreement with the temporally and spatially integrating continuum measurements which give $E_{hot} \cong$ 400 J; $E_{hot} / E = 0.015$ as well as with the hot electron fraction and energy estimated from the measurements of the Raman scattered light. From the Manley-Rowe relations we can calculate the energy in suprathermal electrons from SRS [8,9]. For these experiments we measured simultaneously with x-ray spectroscopy a total energy loss into SRS of 1 kJ. The energy of the scattered photons by SRS is found from the measured spectra so that we can infer the energy into hot electrons of $E_{hot} \cong 410$ J which compares well with the above results.

GAS BAG BENCHMARKING EXPERIMENTS

To validate kinetic code calculations (or collisional-radiative modeling) of atomic spectra, well diagnosed plasmas which can serve as test beds are a necessary prerequisite. At Nova, spherical gas bag plasmas [20] have been developed for laser plasma interaction studies in large scale-length plasmas with typical electron densities of 10^{21} cm^{-3} and peak electron temperatures of 3 keV. The targets consist of an aluminum washer covered with two thin polyimide membranes on either side. By filling the target with 1 atm of propane (C_3H_8) or neopentane (C_5H_{12}) with a small amount of argon (1%) for spectroscopy, an almost spherical gas balloon with a known electron density and of 2.75 mm diameter is created. Figure 6 shows a picture of the target. In the figure, vertical slits can be seen which have been mounted for spatially resolving x-ray spectroscopic measurements.

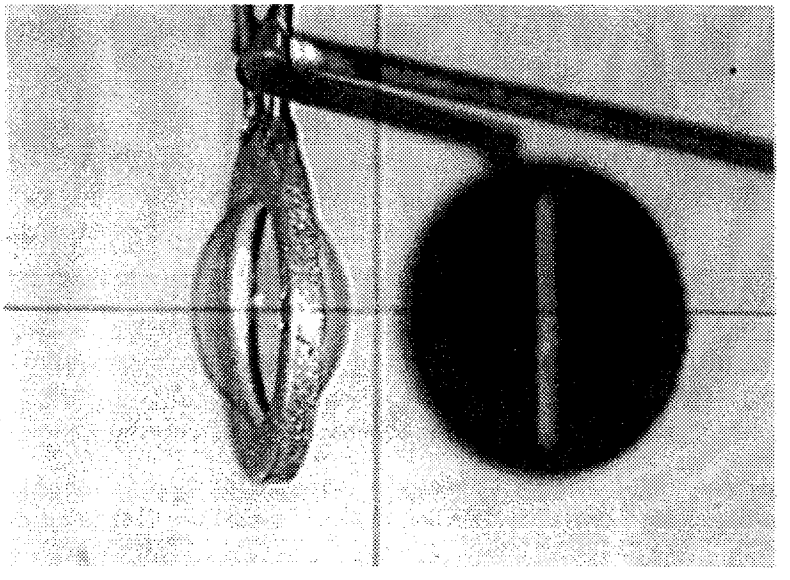

Figure 6. Gas bag target of 2.75 mm diameter together with vertical slits for spatially resolving x-ray spectroscopic measurements.

The gas bags are heated with nine laser beams with a total of 22 kJ for a duration of 1 ns. X-ray spectroscopy from argon and chlorine impurities has been applied to determine the electron temperature in these plasmas and a peak value of 3 keV [22] was measured consistent with radiation hydrodynamic modeling.

Recently, we have performed Thomson scattering and we verified the plasma temperatures measured with x-ray spectroscopy. Thomson scattering observes the scattering of electromagnetic radiation from a probe laser by the electrons of the plasma. It is a spatially and temporally resolving technique which interpretation is based on theory. In the collective scattering regime, where the wavelength of the probe laser is larger than the Debye screening length, the collective behavior of the plasma is observed. In this case, the light is scattered at the ion acoustic and electron plasma wave resonances, and from the measured frequencies and damping of these features - called ion feature and electron feature - one obtains the electron temperatures T_e and densities n_e, ion temperatures T_i, and the averaged ionization stage Z. The macroscopic flow velocities **v** can be inferred from the Doppler shift of the experimental spectra. We applied this powerful diagnostic at Nova using a 4ω probe laser of 50 J energy focused into the gas bag plasma at a distance of 800 μm from the target center. Figure 7 shows an experimental Thomson scattering spectrum of the ion feature. The spectrum was measured temporally resolved with an optical streak camera and a 1m spectrometer. A fit to the experimental data using the theory for multi-ion species [23,53] gives $T_e = 2$ keV and $T_i = 0.6$ keV.

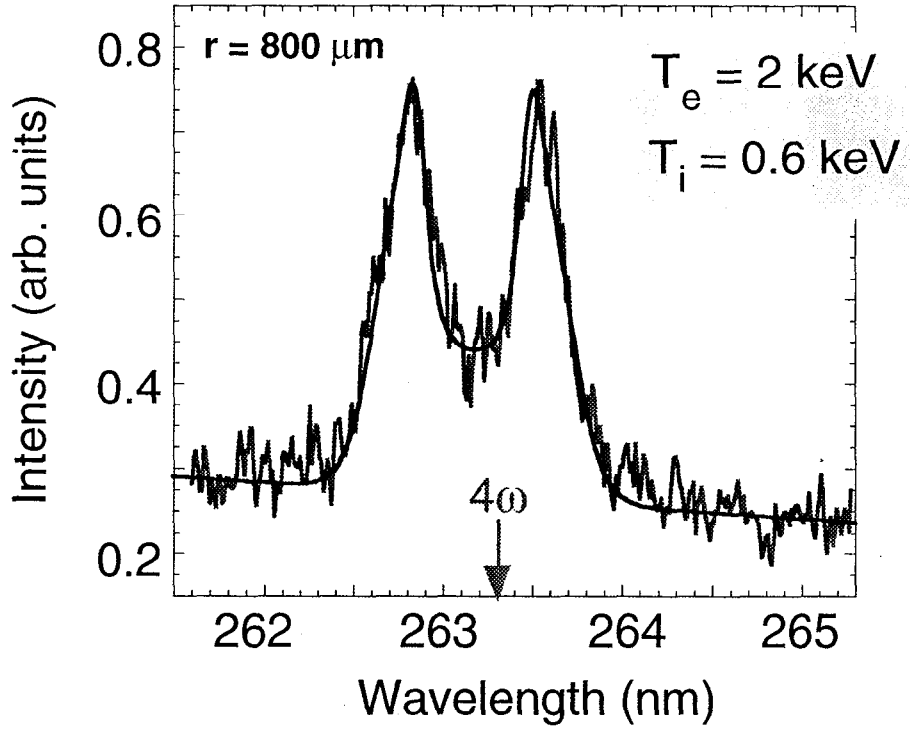

Figure 7. Experimental Thomson scattering spectrum from a gas bag plasma measured at $t = t_0 + 1.2$ ns after the beginning of the 1 ns heater pulse of squared intensity shape.

The experimental electron temperatures show mutual agreement between the results from the Thomson scattering technique and with temporally and spatially resolved x-ray spectroscopy using the intensity ratio of the He-α line to the lithium-like jk l dielectronic satellites. This intensity ratio has many advantages over other spectroscopic techniques: the lines can easily be made optically thin by adjusting the impurity concentrations; the lines are separated only by a small wavelength interval so that the sensitivity of the instrument does not change drastically reducing errors due to the relative calibration; and the upper states of the dielectronic satellite transitions are populated on time scales of ~100 ps so that there are only small differences in the time-resolved and steady state analysis of the spectra reducing possible errors even further. The two techniques are compared in Fig. 8 together with LASNEX simulations. The error bars for the spectroscopic data are in the range of 20% and Thomson scattering data are accurate to within 10%. The experimental data are also in reasonable agreement with the simulations when including heater beam backscattering losses by SBS and SRS. The latter show slightly higher peak temperatures and also a faster rise of the electron temperature than experimentally observed. At present, we are working on improved simulations to take better into account the geometry of the heater beams.

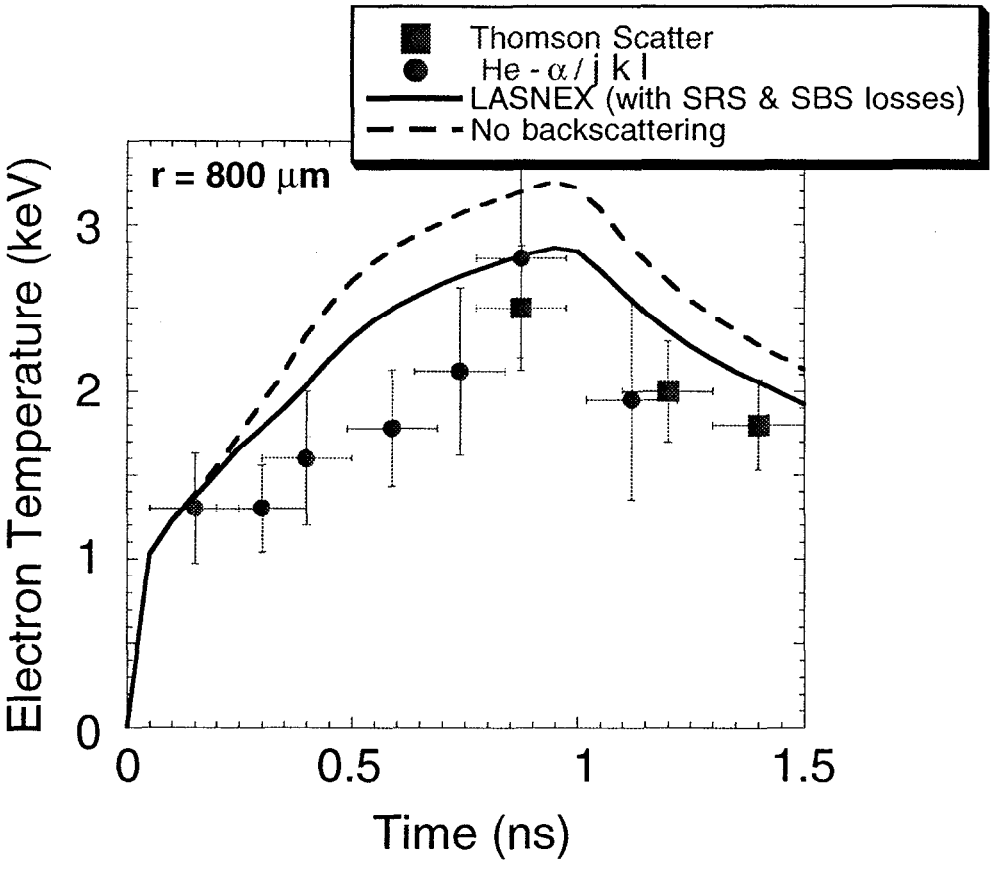

Figure 8. Comparison of simulated and experimental electron temperatures measured temporally resolved with Thomson scattering and x-ray spectroscopy.

While the electron and ion temperature in these gas bag plasmas is well known from the measurements described above the electron density is principally known by the density of the gas fill. Measurements of the wavelength of the Raman scattered light which occurs at the frequency of the electron plasma or Langmuir wave give a value for the electron density which is consistent with the gas fill density [20,24]. In addition, x-ray spectroscopic measurements of the resonance and intercombination line of helium-like argon have also been shown to be in agreement with the expected densities [22]. The detailed measurements and the simulations provide a good understanding of the plasma conditions in these gas bag target and it can therefore be used as a spectroscopic source to benchmark kinetics with experimental spectra. These type of experiments begun two years ago investigating Xe L-shell spectra [54].

Recently, we have measured the dielectronic satellites on the red wing of the He-β line of argon which relative intensity is sensitive to the electron temperature and therefore important for the characterization of capsule implosions [18]. Figure 9 shows an example of a measured spectrum of the He-β line from a gas bag plasma where the satellites are labeled following Ref.[55].

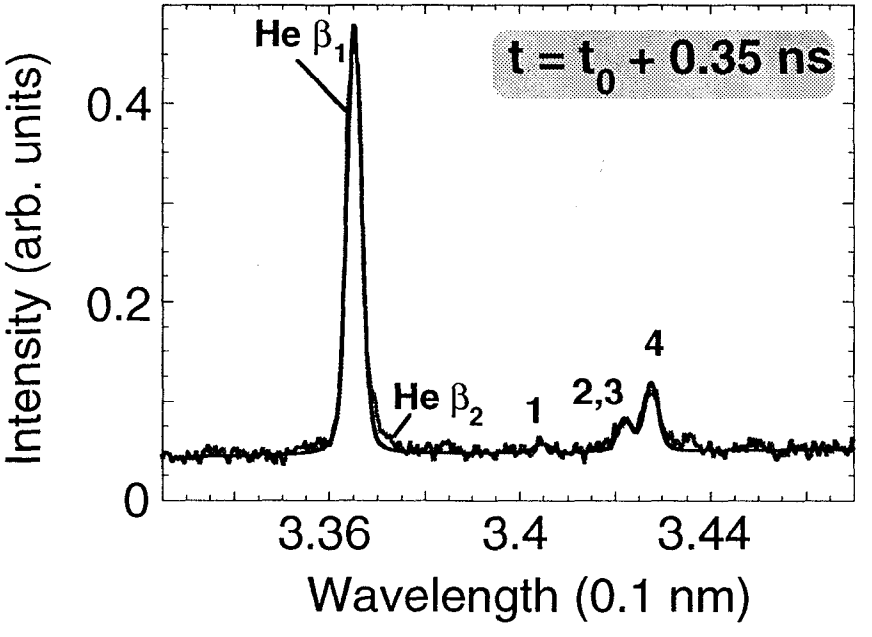

Figure 9. Experimental spectrum of the He-β line of argon from a gas bag plasma where n_e and T_e is determined by independent measurements such as Thomson scattering.

The spectrum has been fit by Voigt profiles to determine the relative intensities of the lines (the He-β_2 component is excluded from the fit to show its small contribution to the intensity of the He-β line but it is included when comparing with

calculated line ratios). For example the experimental ratio between the satellite feature 4 and the He-β line is 0.15 ± 0.01 for $n_e = 10^{21}$ cm^{-3} and $T_e = 1.3$ keV. This result is in excellent agreement with collisional radiative modeling which predict a ratio of 0.17. The complete spectrum is presently under investigation. In particular, the consistency of the various line ratios with the code predictions for a single temperature and density are being studied. In addition, data have been taken at various times during the gas bag heating and for different densities. These results will be published elsewhere. The present results verify the collisional radiative modeling which is applied for the interpretation of implosion spectra [18,54]. It indicates that the smaller temperatures (when compared to simulations) obtained for the capsule conditions with this method are not due to the kinetic models. Spatial temperature gradients and/or difficulties with the satellite technique at small intensities and large widths are probably responsible for the discrepancies.

CONCLUSIONS

The present laser absorption measurements at the Nova laser facility are important to understand the physics of closed-geometry gas-filled hohlraums. They were designed to study plasma conditions similar to those anticipated at the National Ignition Facility. For example, laser beam smoothing by kinoform phase plates and by spectral dispersion has been adopted in the NIF design because of its beneficial effects seen in the Nova experiments. Its will be particularly important to suppress stimulated Raman scattering in the large scale plasmas encountered at the NIF because of the production of hot electrons. Our spectroscopic measurements will be a useful tool for future experiments to determine the local fraction of the hot electrons near the fusion capsule to estimate possible preheat effects.

Experiments in well-diagnosed gas bag plasmas have shown that collisional radiative (kinetics) modeling of the intensities of the He-β line and its satellites is in excellent agreement with the measured spectra. This result increases our confidence in the characterization of implosion capsules which requires Stark broadening calculations coupled to a kinetics model to calculate the detailed line shapes for density and temperature diagnostics.

ACKNOWLEDGMENTS

I would like to thank C. A. Back, C. Decker, B. A. Hammel, R. M. Herman, R. W. Lee, B. J. MacGowan, A. Osterheld, and L. J. Suter for helpful discussions. This work was performed under the auspices of the U. S. Department of Energy by the Lawrence Livermore National Laboratory under Contract No. W-7405-ENG-48.

REFERENCES

[1] J. H. Nuckolls, Phys. Today **35**, No. 9, 24 (1982).
[2] J. D. Lindl, Phys. Plasmas **2**, 3933 (1995).
[3] S. W. Haan *et al.*, Phys. Plasmas **2**, 2480 (1995).

[4] W. L. Kruer, *The Physics of Laser Plasma Interactions* (Addison-Wesley, New York, 1988).
[5] T. P. Hughes, *Plasmas and Laser Light* (John Wiley and Sons, New York, 1975).
[6] S. H. Glenzer *et al.*, Phys. Rev. Lett. **80**, 2845 (1998).
[7] J. W. Shaerer *et al.*, Phys. Rev. A **6**, 764 (1972).
[8] K. G. Estabrook *et al.*, Phys. Rev. Lett. **45**, 1399 (1980).
[9] K. G. Estabrook and W. L. Kruer, Phys. Fluids **26**, 1892 (1983).
[10] R. L. Kauffman, in *Handbook of Plasma Physics*, edited by M. N. Rosenbluth and R. Z. Sagdeev, *Physics of Laser Plasma*, edited by A. Rubenchik, and S. Witkowski (North-Holland, Amsterdam, 1991), pp. 111-162.
[11] R. W. Lee *et al.*, J. Quant. Spectrosc. Radiat. Transfer **32**, 91 (1984).
R. W. Lee *private communication* (1997).
[12] H. R. Griem, Phys Fluids B **4**, 2346 (1992).
[13] J. P. Matte *et al.*, Phys. Rev. Lett. **72**, 1208 (1994).
[14] J. Abdallah *et al.*, Phys. Scripta **53**, 705 (1996).
[15] F. B. Rosmej, J. Phys. B **28**, L747 (1995).
F. B. Rosmej, J. Quant. Spectrosc. Radiat. Transfer **51**, 319 (1994).
[16] S. H. Glenzer *et al.*, Phys. Rev. Lett. **81**, 365 (1998).
[17] A. A. Offenberger et al., Phys. Rev. Lett. **49**, 371 (1982).
[18] B. A. Hammel et al., Phys. Rev. Lett. **70**, 1263 (1993).
[19] N. Woolsey et al., Phys. Rev. E **57**, 4650 (1998).
[20] B. J. MacGowan *et al.*, Phys. Plasmas **3**, 2020 (1996).
[21] D. H. Kalanter *et al.*, Phys. Plasmas **2**, 3161 (1995).
[22] S. H. Glenzer *et al.*, Phys. Rev. E **55**, 927 (1997).
[23] S. H. Glenzer *et al.*, Phys. Rev. Lett. **77**, 1496 (1996).
[24] D. S. Montgomery *et al.*, Phys. Plasmas **5**, 1935 (1998).
[25] H. R. Griem *et al.*, Phys. Rev. E **56**, 7186 (1997). (See also these proceedings).
[26] S. Alexiou *et al.*, Phys. Rev. E (Comment), in press (1998).
[27] E. M. Campbell *et al.*, Rev. Sci. Intrum. **57**, 2101 (1986).
[28] M. D. Cable *et al.*, Phys. Rev. Lett. **73**, 2316 (1994).
[29] A. A. Hauer *et al.*, Phys. Plasmas **2**, 2488 (1995).
[30] N. D. Delamater *et al.*, Phys. Plasmas **3**, 2022 (1996).
[31] S. H. Glenzer *et al.*, Phys. Rev. Lett. **79**, 1277 (1997).
[32] S. N. Dixit *et al.*, Optics Lett. **21**, 1715 (1996).
[33] Y. Kato *et al.*, Phys. Rev. Lett. **53**, 1057 (1985).
[34] D. M. Pennington *et al.*, Proc. SPIE **1870**, 175 (1993).
[35] R. H. Lehmberg and S. P. Obenschein, Opt. Commun. **46**, 27 (1983).
[36] S. Skupsky *et al.*, J. Appl. Phys. **66**, 3456 (1989).
[37] H. Kornblum *et al.*, Rev. Sci. Instrum. **57**, 2179 (1986).
[38] G. B. Zimmerman and W. L. Kruer, Comments Plasma Phys. Controlled Fusion **2**, 85 (1975).
[39] L. J. Suter *et al.*, Phys. Rev. Lett. **73**, 2328 (1994).
[40] L. J. Suter *et al.*, Phys. Plasmas **3**, 2057 (1996).
[41] R. E. Marshak, Phys. Fluids **1**, 24 (1958).
[42] R. Sigel *et al.*, Phys. Rev. Lett. **65**, 587 (1990).
[43] H. Nishimura *et al.*, Phys. Rev. A **44**, 8323 (1991).
[44] R. L. Kauffman *et al.*, Phys. Rev. Lett. **73**, 2320 (1994).

[45] C. Decker *et al.*, Phys. Rev. Lett. **79**, 1491 (1997).
[46] R. E. Turner *et al.*, *submitted to* Phys. Rev. Lett. (1998).
[47] R. K. Kirkwood *et al.*, Rev. Sci. Instrum. **68**, 636 (1997).
[48] E. M. Epperlein and R. Short, Phys. Fluids B **4**, 2211 (1992).
[49] R. L. Berger *et al.*, Fluids B **5**, 2243, (1993).
[50] R. Sigel *et al.*, Phys. Rev. A **38**, 5779 (1988).
[51] A. H. Gabriel, Mon. Not. R. Astron. Soc. **160**, 99 (1972).
[52] C. A. Back *et al.*, Phys. Rev. Lett. **77**, 4350 (1996).
[53] D. E. Evans, Plasma Phys. **12**, 573 (1970).
[54] C. A. Back *et al.*, in *Spectral Line Shapes*, edited by M. Zoppi and L. Ulivi, Vol. 9 (AIP Conference Proceedings 386, New York, 1997), pp. 35-44.
[55] P. Beiersdorfer *et al.*, Phys. Rev. E **52**, 1980 (1995).